Structural and Multidisciplinary Optimization manuscript No.
(will be inserted by the editor)

Obtaining a Hyperelastic Non-Linear Orthotropic Material Model via Inverse Bubble Inflation Analysis

Charles F. Jekel · Gerhard Venter · Martin P. Venter

Received: September 14, 2015 / Revised February 3, 2016 / Accepted: April 6, 2016

The final publication is available at Springer via http://dx.doi.org/10.1007/s00158-016-1456-8.

Abstract An inverse bubble inflation test is proposed utilizing full displacement field matching to obtain non-linear material models suitable for the Finite Element (FE) method. In this paper a known non-linear orthotropic material model is assumed as the solution for the inverse method to illustrate the process. A bubble inflation FE analysis is performed with the known material model to determine the load and displacement field from the assumed material. Polynomial surfaces are fit to the nodal displacement values of the FE model, such that the entire displacement field is stored as three unique polynomial surfaces. An error formulation was established to quantify the quality of fit between different bubble inflation displacement fields. Gradient based optimization is used to obtain the assumed material model by matching the full displacement field. The inverse bubble inflation test successful produces a non-linear orthotropic model that is analogous to the assumed non-linear orthotropic material, and thus demonstrates that the inverse bubble inflation analysis would be able to characterize other non-linear orthotropic materials.

Keywords FE analysis · material model · gradient optimization · non-linear orthotropic · inverse bubble inflation

Research funded by Wilhelm Frank Trust

Corresponding Author: Charles F. Jekel

C.F. Jekel · G. Venter · M.P. Venter
Stellenbosch University
Department of Mechanical and Mechatronic Engineering
Private Bag X1, Matieland, 7602 Tel.: +27-021-8084145
E-mail: cjekel@gmail.com, gventer@sun.ac.za, mpventer@sun.ac.za

1 Introduction

Membrane structures designed with technical woven textiles, coated fabrics, and various polymer membranes are often operated in the non-linear region, thus it is anticipated that the material model should be able to replicate the non-linear behavior of the material. An inverse bubble inflation method may improve the homogenization of the material due to the complex load state experienced as the material deforms. However, a mechanism for obtaining material models utilizing the inverse method with a bubble inflation test has not yet been established. This paper proposes the procedure for obtaining a non-linear orthotropic material model from an inverse bubble inflation test. The results of a non-linear Finite Element (FE) analysis of a bubble inflation test are used instead of experimental data from a physical bubble test. The non-linear orthotropic material model used in the bubble inflation FE analysis is assumed to be the solution. To demonstrate the capability of the inverse bubble inflation test, it is shown that the method can reproduce an analogous non-linear orthotropic model from the assumed non-linear orthotropic material. This suggests that the inverse bubble inflation test can successfully determine a non-linear orthotropic material model from a bubble inflation test on non-linear orthotropic material.

The FE method has been an important tool used in the design and analysis of structures. The accuracy of these models depends largely on the ability of the material model to replicate the physical response of the material. Obtaining an accurate material model has been the topic of many research projects. These material models can be described by one of two broad categories: micromechanical or macromechanical. Micromechanical material models analyze the complex in-

teraction of the material. For an entire fabric structure, a micromechanical model will include the interactions between individual yarns. While there is benefit to this high level of fidelity, it is also highly impractical for modeling an entire structure as the model becomes too computationally expensive (Cavallaro et al 2003).

Macromechanical models assume the material to be of a single continuum, for which the constitutive relationships can be determined from material testing. Often uniaxial and biaxial tests are performed on the material, in which case the experimental stress/strain relationship is used to characterize the material. An example of a macromechanical material model would be the plane stress constant thickness orthotropic model. This model has been commonly used, for membrane structures, because of the model's ability to exhibit direction dependent stiffness. Four constants are needed to define the material model, the Young's moduli in the primary and secondary direction (E_1, E_2), Poisson's ratio (ν_{12}), and Shear modulus (G_{12}). In some cases, a non-linear material model can more accurately characterize the physical behavior of a material.

The use of a non-linear orthtropic material model for PVC-coated polyester was -demonstrated by Ambroziak and Kłosowski (2014). Both uniaxial and biaxial tensile tests were conducted. Stress strain curves were calculated in both material directions from these tests. While the resulting relationship was highly nonlinear, it was observed to be approximated well by a piece-wise linear function. A tri-linear orthotropic material model was purposed. Fundamentally this material model is a plane stress linear orthotropic material model. Though three different Young's moduli, for both E_1 and E_2, are defined each for a particular strain region. Then once the element exceeds this strain region, a new Young's modulus is assigned. The result is a simple non-linear material model which correlated well with the experimental data.

There are direct and inverse methods for obtaining material models. The method utilized by Ambroziak and Kłosowski (2014) is a direct method. A physical test is conducted to determine the material's constitutive relationship. The resulting experimental relationship is then passed directly into the material model for an FE analysis replicating the testing conditions. Ideally, it is then shown that the material model is capable of replicating the behavior of the physical test.

The inverse method is fundamentally different from the direct method. With the inverse method, an FE analysis is created replicating the conditions of the physical test first. Optimization is then used to determine the best material model parameters by minimizing the difference between the FE analysis and the physical test. While each method has advantages, the inverse method may reduce the engineering time required to create material models suitable for FE analysis. More importantly, the material is characterized with a load state that is more complex than traditional uniaxial or biaxial testing. This added complexity may be more representative of reality. Materials such as technical woven textiles or coated fabrics violate continuum mechanics in a macro sense as the material is not represented by a single continuum. Thus the homogenization of the material into discrete elements for use in the FE method may be a cumbersome task. The inverse method is capable of determining the best homogenized FE material model representative of a complex load state.

Garbowski et al (2011) used the inverse method to characterize paper by performing biaxial tests on paper. A circular hole was cut in the center of the biaxial test sample to increase the inhomogeneous response field. Digital Image Correlation (DIC) was used to capture the full field displacements of the test samples. The physical test was reproduced in an FE analysis. The deformation of the cruciform specimen is then compared to the nodes of the FE model. An elastic-plastic orthotropic material model was thus determined with much success by optimizing the parameters of the material model, minimizing the differences between the FE model and the deformations of the test specimen. In the end a software package was created suitable for determining the constitutive relationship of test specimens that can be performed on a portable computer.

Bubble inflation tests are a popular method for introducing an equal biaxial load case, especially in cases where very large deformations may inhibit the ability for a conventional biaxial test. The bubble inflation tests have been used to characterize polymers such as Ethylene Tetra Fluoro Ethylene (ETFE) and even flour/water dough. A bubble inflation test involves clamping a material sample to a flat plate with a circular clamp. A medium is then introduced on one side of the material, which applies a load to the material. The material inflates from the pressure, creating a bubble shape seen in Fig 1. Image tracking techniques, such as DIC can be used to track the deformation of the material as it inflates. Previous literature has assumed the resulting bubble to be spherical in shape. Reuge et al (2001) and Charalambides et al (2002) used a single camera to measure the bubble height, while Galliot and Luchsinger (2011) used a two camera DIC setup. Assuming that the material is incompressible, it is possible to approximate the strain utilizing the height of the bubble and the initial bubble radius. Pressure ves-

sel theory is used to calculate the stress. This results in a stress strain relationship for a 1:1 biaxial load case.

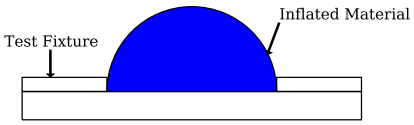

Fig. 1 Inflated material in a bubble test fixture

This paper proposes the use of an inverse bubble inflation test for obtaining non-linear orthotropic material models. The procedure for obtaining the material model via inverse bubble inflation technique is outlined. The results of an FE analysis with an assumed material model are used as a substitute for the experimental bubble inflation test data. This is done to demonstrate that the method is capable of finding the correct material model parameters. If the material model obtained from the inverse bubble procedure is analogous to the known starting point, it can be concluded that the inverse bubble inflation technique is a valid method for characterizing non-linear orthotropic models from non-linear orthotropic materials.

The inverse bubble inflation method to obtain material models is intended for thin membrane material used in inflatable structures or structural membranes. However the method is not limited to just membrane materials, but could be used to investigate other material that could be appropriately described by a thin shell or membrane element formulations. The method utilizes just a single test to characterize non-linear orthotropic materials.

2 Methodology

It is important to understand the effectiveness of the inverse bubble inflation method for an ideal test scenario before attempting the technique on physical test data. A large number of factors may influence the ability to obtain an accurate material model, or otherwise prove the inverse method impractical. Thus to demonstrate the ability of the inverse bubble inflation test to reproduce the material models from an assumed ideal material, demonstrates that the technique is capable of producing accurate material models. Once this has been demonstrated the test method may be suitable for characterizing material models from physical tests.

A non-linear FE model representing the physical response of the bubble test was created using MSC Marc (2014). The model comprises of 800 linear quad elements arranged in a circle that is 200 mm in diameter, as seen in Fig. 2. The appropriate mesh size was determined by an initial mesh convergence study. Pin constraints are applied around the edge of the circle. A linear pressure ramp of 300 kPa is applied to all of the elements, which represents the load from the inflated medium as a function of time. Upon completion of the FE simulation, the node data is exported at pressures of interest for the error calculation.

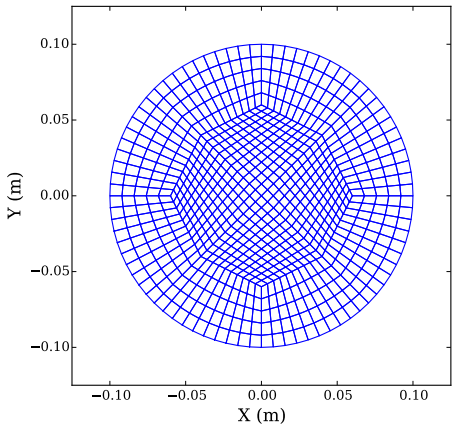

Fig. 2 Mesh used for the bubble inflation FE model

MSC Marc (2014) includes a material model, the NLELAST model definition, capable of creating a simplified non-linear elastic orthotropic material model. The model is a hyperelastic planar orthotropic material model. The material model is capable of producing a directional dependent non-linear load elongation curve. In addition the material model contains no plasticity, so the model is fully recoverable when unloaded. The Young's moduli (E_1 , E_2), Poisson's ratio (ν_{12}), and shear modulus (G_{12}) can be defined as functions of the strain component in their respective direction. During deformation, the material model iterates the elemental strain components in order to assign the appropriate orthotropic moduli to the element. To add complexity to the inverse bubble inflation test, third order polynomials are chosen for each of the moduli as seen in Eqs. 1 - 3. Demonstrating the success of the inverse bubble inflation test on this highly non-linear material model suggest that the inverse method may be just as successful with simpler material models. The stress output of such a model may be non-sensible as the model may violate the constitutive relationships of traditional FE theory. However, such material models may still be

useful in the design/analysis of structures by accurately predicting the load displacement behavior.

$$G_{12}(\gamma_{12}) = \beta_0\gamma_{12}^3 + \beta_1\gamma_{12}^2 + \beta_2\gamma_{12} + \beta_3 \quad (1)$$

$$E_2(\epsilon_2) = \beta_4\epsilon_2^3 + \beta_5\epsilon_2^2 + \beta_6\epsilon_2 + \beta_7 \quad (2)$$

$$E_1(\epsilon_1) = \beta_8\epsilon_1^3 + \beta_9\epsilon_1^2 + \beta_{10}\epsilon_1 + \beta_{11} \quad (3)$$

A mesh convergence study determined that the 800 element mesh produced acceptable displacement error while having a low cost computational run time. The mesh size used is largely dependent upon the computational resources available and desired accuracy. Since the optimizer will call the FE model for each function evaluation, reducing the FE model run time greatly reduces the optimization time. To avoid a mesh sensitive optimization result, it is recommended to perform an initial mesh convergence study. The mesh convergence study showed the 800 element mesh to produce displacements values nearly identical to finer meshes. The maximum displacement value was within 0.05 percent for mesh sizes of 800 and 831,472 elements.

The sensitivity of the FE model to Poisson's ratio was investigated. The FE bubble inflation model was run with different Poisson's ratios for the same non-linear moduli (E_1 , E_2, & G_{12}). The resulting maximum displacement values were normalized to the set's average, and can be seen in Fig. 3 for Poisson's ratios ranging from 0.05 to 0.45. It is observed that for the same non-linear moduli, the Poisson's ratio varied the maximum displacement value by plus or minus three percent. It was determined that the Poisson's ratio was not a significant contribution to the FE bubble inflation model. Thus the Poisson's ratio was held constant, and not included as a variable for optimization.

Vanderplaats Research & Development Inc. (2001) Design Optimization Tools (DOT) was the optimization library used in the inverse method. DOT is a multipurpose gradient based software library designed for engineering applications. Gradient based optimization proved to be a sufficient optimization method in demonstrating the effectiveness of the inverse bubble test. The constrained gradient optimization algorithm used was the Modified Method of Feasible Directions (MMFD). A simple python script interfaces with DOT and the MSC Marc input file of the bubble model. The material model variables (β_0 - β_{11} of Eqs. 1 - 3) are fed into DOT as variables to optimize. The optimization goal is to minimize the error between the FE model bubble displacements and the known displacements. This

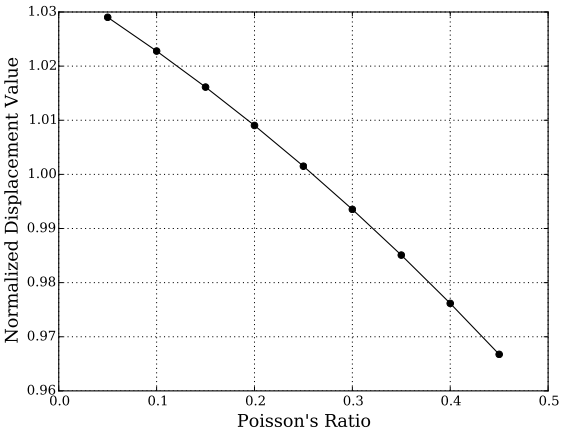

Fig. 3 Normalized maximum displacement value of FE bubble inflation model for various Poisson's ratios

is subjected to two constraints. The first being that the moduli must remain above zero for the strain range of the material model. The second constraint ensures that non-linear FE analysis produces a valid exit code, as some set of material model parameters may generate convergence problems. DOT was designed to be useful as an engineering optimizer, so the algorithm attempts to stay in the feasible region as much as possible in one dimensional searches.

3 Surface Fitting

The assumed non-linear orthotropic material model derives from physical tests on PVC-coated polyester. The β terms in Eqs. 1-3 were fit to the uniaxial test data in the primary, secondary, and 45-bias directions. A plot of the three moduli limited to their strain component can be seen in Fig. 4. The magnitude and nonlinearilty of E_1 dominates the other moduli. It can be noted that it is possible to simplify the moduli to a lower order polynomial as the curves do not represent a third order polynomial, but solving the variables of the third order polynomial adds additional complexity for the optimization problem and better demonstrates the effectiveness of the inverse method. A Poisson's ratio of 0.24 was used, which is similar to the Poisson's ratio used for various PVC-coated polyesters by Galliot and Luchsinger (2009) in a standard orthotropic model. The FE bubble inflation model is run with this assumed material model, simulating a physical bubble inflation test on PVC-coated polyester. Each curve in Fig. 4 ends at the maximum strain component value as experienced by the FE bubble model. The result of the analysis will be used instead of experimental bubble

test data to demonstrate the effectiveness of the inverse bubble inflation test.

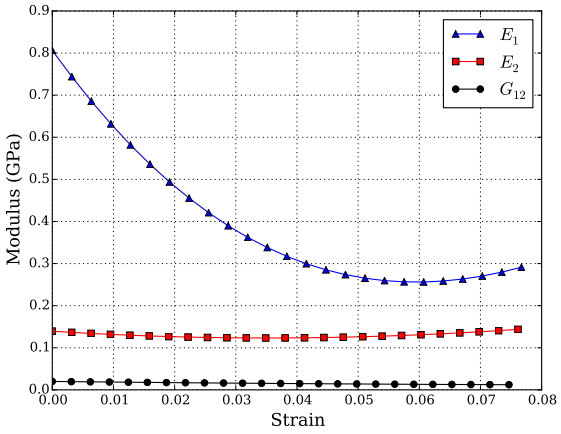

Fig. 4 Non-linear orthotropic material model moduli as functions of strain

Three separate polynomials are fitted to the nodal displacement values at seven unique pressure instances of the inflating FE model. All of the nodes of the mesh prior to inflation lie in the XY plane. Thus each node will have a unique displacement value as a function of it's original XY location. The least squares method is used to fit a fourth order polynomial surface to the node locations for the displacement values in the X, Y, and Z directions. It was found that a fourth order polynomial, defined by 25 coefficients and shown in Eq. 4, to be the best fit. The fitted surfaces along with the nodal displacement values can be seen in Figs. 5 - 7.

$$\begin{aligned} F(X,Y) = {} & C_0X^4Y^4 + C_1X^3Y^4 + C_2X^2Y^4 + C_3XY^4 + \\ & C_4Y^4 + C_5X^4Y^3 + C_6X^3Y^3 + C_7X^2Y^3 + \\ & C_8XY^3 + C_9Y^3 + C_{10}X^4Y^2 + C_{11}X^3Y^2 + \\ & C_{12}X^2Y^2 + C_{13}XY^2 + C_{14}Y^2 + C_{15}X^4Y + \\ & C_{16}X^3Y + C_{17}X^2Y + C_{18}XY + C_{19}Y + \\ & C_{20}X^4 + C_{21}X^3 + C_{22}X^2 + C_{23}X + C_{24} \end{aligned} \tag{4}$$

The entire nodal displacements of the bubble inflation FE model can be represented by a series of polynomials, as a function of the original nodal XY coordinates, at different inflation pressures. The polynomials are exceptional fits to the nodal X, Y, and Z displacements. The coefficient of determination for each polynomial was greater than 0.999 as seen in Table 1. A comparison of the fitted displacement Z values from the

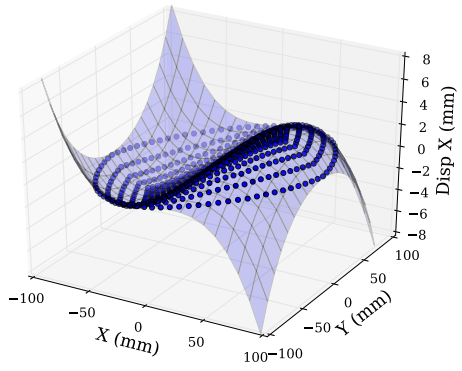

Fig. 5 Nodal displacement X values on the fitted fourth order polynomial surface at 300 kPa

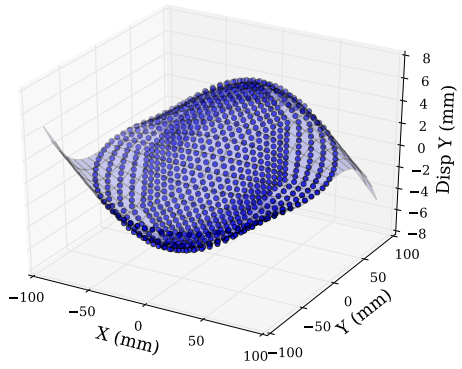

Fig. 6 Nodal displacement Y values on the fitted fourth order polynomial surface at 300 kPa

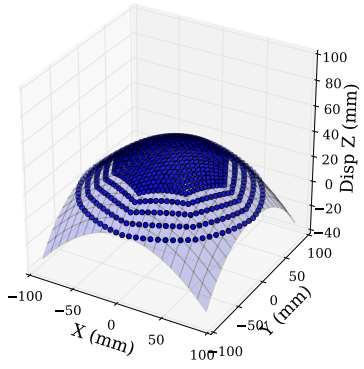

Fig. 7 Nodal displacement Z values on the fitted fourth order polynomial surface at 300 kPa

fitted polynomial and the known displacement Z values is seen in Fig. 8. The fitted polynomial and known displacement values are nearly identical.

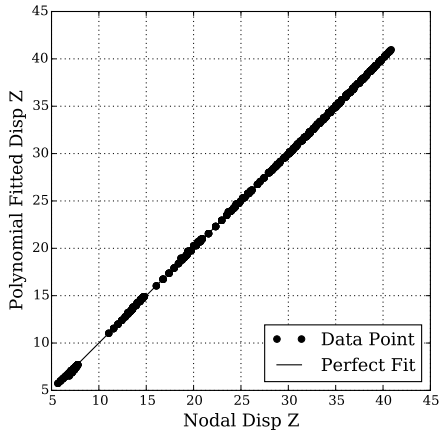

Fig. 8 Disp Z nodal values against the Disp Z polynomial fitted values at 300 kPa

Table 1 Coefficient of determination for the polynomials used to define the bubble displacements

Pressure (kPa)	R^2 Disp X	R^2 Disp Y	R^2 Disp Z
22	0.99999	0.99971	0.99999
59	0.99999	0.99980	0.99999
97	0.99998	0.99994	0.99999
132	0.99994	0.99989	0.99999
186	0.99986	0.99970	0.99998
251	0.99967	0.99901	0.99994
300	0.99962	0.99836	0.99994

Utilizing polynomials to represent the FE model adds simplicity to the inverse method. Only the coefficients of the polynomials need to be stored, as opposed to the entire nodal displacement values. The error formulation minimizes the difference in the full field nodal displacement values. The correct displacement values can be calculated by simply evaluating a polynomial. These are then compared with the nodal displacements of a new FE run to evaluate the error from a new material model.

A DIC setup using at least two cameras is capable of accurately providing the full three dimensional displacement field on a physical bubble inflation test. It can be cumbersome setting up the DIC to calculate displacement values at the exact node locations of the FE model. Instead of mapping the DIC displacement values to specific node locations, a polynomial surface of best fit is used. These polynomials can be arranged such that the axes align with that of the FE mesh. Then the polynomial can be evaluated at the FE model's node locations to compare the displacement results of the FE model and the physical test. Additionally the polynomials represent a smooth surface to match the full displacement field to the FE model. This smooth surface eliminates noise in test data that may result from the DIC calculated displacement data. Thus the inverse bubble inflation test can be utilized on physical test data easily by swapping the current displacement polynomials with displacement polynomials from a physical test.

The inverse bubble inflation test was first attempted by only matching the nodal Z values of the FE models. It was then discovered that the physical shape was non-unique to the material model. This was because very different non-linear material models could reproduce a nearly identical inflated bubble shape. Instead, by matching the full displacement field (X, Y, and Z displacements) it is ensured that a unique solution is achieved.

4 Optimization

Optimization is the mechanism used by the inverse method to determine material models. The optimum material model is determined from gradient based optimization on random starting points. The FE analysis results for a particular set of material model parameters is compared against the assumed material model, utilizing a single objective function. An objective function value of 0.0 represents that the exact displacement field was produced. This objective function is minimized until a local minimum has been found. Multiple gradient optimizations are run simultaneously from random starting points to determine the global minimum, which represents the material model determined by the inverse bubble inflation test.

4.1 Objective Function

Root mean square (RMS) error is used to evaluate how well the FE analysis of a particular material model matches with the known solution. The error can be represented by a single value for each FE analysis. This single value is minimized as the optimizer searches for the ideal material model.

At each of the seven pressures for which polynomials were fitted to the bubble inflation model (see Table 1), three RMS errors are calculated. One for each nodal displacement direction. The fitted polynomials (which could represent experimental bubble inflation

displacement data, but in this case represents the assumed non-linear orthotropic material model) are the terms P_X, P_Y, and P_Z. The results of the FE model nodal displacements for a new material model are the terms d_X, d_Y, and d_Z. Both the polynomials and the displacements are functions of pressure p, as there is a unique set of polynomials and displacements for each of the seven pressures of interest. The root mean square errors for the three directions are seen in Eqs. 5 - 7 as functions of pressure, where n represents the total number of nodes.

$$e_X(p) = \sqrt{\frac{\sum_{i=1}^{n}(d_{Xi}(p) - P_{Xi}(p))^2}{n}} \tag{5}$$

$$e_Y(p) = \sqrt{\frac{\sum_{i=1}^{n}(d_{Yi}(p) - P_{Yi}(p))^2}{n}} \tag{6}$$

$$e_Z(p) = \sqrt{\frac{\sum_{i=1}^{n}(d_{Zi}(p) - P_{Zi}(p))^2}{n}} \tag{7}$$

In total, 21 different root mean square errors are calculated for the three directions at seven different pressures. A single error value which represents the overall fit between the FE bubble inflation model and the assumed material can be created by simply summing up all of the root mean square errors. However this introduces bias into the objective function. The FE bubble model is inflated in the Z direction, thus it is anticipated that the nodal displacements will always be larger in the Z direction as opposed to the X and Y displacements. In an effort to reduce this bias, each root mean square error is normalized by the maximum polynomial value at the corresponding pressure. The result is a summation of equally weighted errors seen in Eq. 8. Thus e represents a single value that describes the entire fit between the known non-linear orthotropic material and the attempted material model.

$$e = \sum_{i=1}^{p} \frac{e_X(i)}{\max(P_X(i))} + \frac{e_Y(i)}{\max(P_Y(i))} + \frac{e_Z(i)}{\max(P_Z(i))} \tag{8}$$

The overall objective function of the optimization can be expressed by minimizing the overall error of the FE model's results for a particular material model. This is subjected to two constraints, the first being that the moduli in the material model remain positive for their entire strain limit. The second being that the FE analysis is valid, in which case Marc outputs an exit code of 3004. The objective function can be seen in Eq. 9. The two constraints serve as logical flags for the constrained optimization. When a constraint is violated, a value of 1 is fed into the algorithm, while a value of -1 indicates a satisfied constraint. This type of true-false boolean constraint may be problematic for a gradient based optimization algorithm, however DOT deals with boolean constraints well by backtracking when encountering a violated constraint in the one dimensional search. It is important to mention that DOT's approach works well, provided that the optimization is started from a feasible point.

$$\begin{aligned} &\text{minimize:} \quad e \\ &\text{such that:} \quad E_1, E_2, G_{12} > 0 \quad \text{and} \\ &\qquad\qquad \text{Marc Exit Code} = 3004 \end{aligned} \tag{9}$$

4.2 Procedure

Multiple optimizations are run to ensure that the best material model is found. Fifty starting points are generated at random between the upper and lower bounds. Each starting point, is then run through the bubble inflation FE analysis to ensure the constraints are satisfied. If a constrained is violated for a particular starting point, a random starting point is generated between the bounds. This process is repeated until each starting point begins in the feasible region. It is ensured that each starting point satisfies the constraints, because the DOT optimizer cannot start with a violated true-false constraint. The assumed non-linear orthotropic material model variables chosen and optimization bounds are listed in Table 2. These bounds were chosen to be an order of magnitude in size, with the non-linear orthotropic variables appearing somewhere in-between the bounds. If the solution is unknown, appropriate bounds may be chosen around the result of a single initial optimization. Random starting points were found easier to generate than starting points selected from a latin hypercube sampling that reside in the feasible region. Often a set of starting points, generated from a latin hypercube sampling, included a point that violated one of the constraints. In order to overcome the violated constraint, a new latin hypercube sampling was generated. The repeated formation of latin hypercube starting points was found more computationally intensive than obtaining starting points generated from random to reside in the feasible region. All 50 optimizations are run simultaneously with the MMFD algorithm. The material model determined from the inverse method has the lowest found objective function.

Table 2 Variables and bounds used for the non-linear orthotropic material model

Variable	Assumed Value	Lower Bound	Upper Bound
β_0	-7.96788×10^{-3}	-1.0×10^{-2}	0.0×10^{0}
β_1	7.10747×10^{-1}	0.0×10^{0}	1.0×10^{0}
β_2	-1.56912×10^{-1}	-3.0×10^{-1}	0.0×10^{0}
β_3	2.00439×10^{-2}	7.0×10^{-3}	7.0×10^{-2}
β_4	-1.06241×10^{1}	-1.0×10^{3}	1.0×10^{2}
β_5	1.37830×10^{1}	-1.0×10^{1}	1.0×10^{2}
β_6	-9.31830×10^{-1}	-1.0×10^{1}	1.0×10^{0}
β_7	1.39437×10^{-1}	5.0×10^{-2}	5.0×10^{-1}
β_8	-4.79622×10^{2}	-1.0×10^{3}	0.0×10^{0}
β_9	2.12650×10^{2}	0.0×10^{0}	7.0×10^{2}
β_{10}	-2.02028×10^{1}	-7.0×10^{1}	0.0×10^{0}
β_{11}	8.06350×10^{-1}	2.5×10^{-1}	1.5×10^{0}

The majority of the DOT parameters are utilized in their default configuration. This includes DOT's variable scaling, gradient step size, and convergence settings. The overall optimization process is well suited for parallel computing as the 12 variable gradient search may be performed at the same time. In addition multiple cores can be used in the FE bubble inflation analysis.

5 Results

All 50 optimizations were performed in parallel. The optimum determined from each optimization can be seen in Fig. 9, sorted from the worst objective value found to the best. The result of each optimization represents a local minimum that was found in the design space. It is important to note that no two optimizations found the exact same optimum material model. More than half of the optimizations resulted in an objective value less than 0.5, in which an objective of zero represents a material model that produces the exact same displacement field as the assumed non-linear orthotropic material. These low objective functions suggest that resulting material models produce nodal displacements similar to the assumed material. While the design space does not appear to be flat, having multiple local minimum near zero suggests that the problem is well posed.

The material models determined through the optimization are similar to the assumed non-linear orthotropic material. The material models resulting from the top 10 percent of optimizations, alongside the assumed material model is seen in Fig. 10. The variance between moduli curves ultimately does not impact the FE model as the full displacement fields are similar based upon the low objective values.

The best material model parameters produce a displacement field that is nearly identical to the assumed

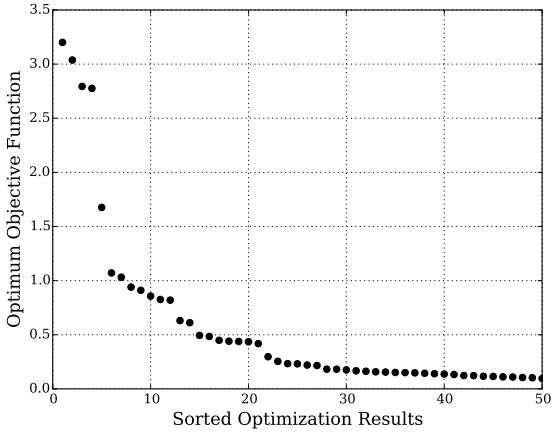

Fig. 9 Sorted optima of optimization results from 50 random starting points

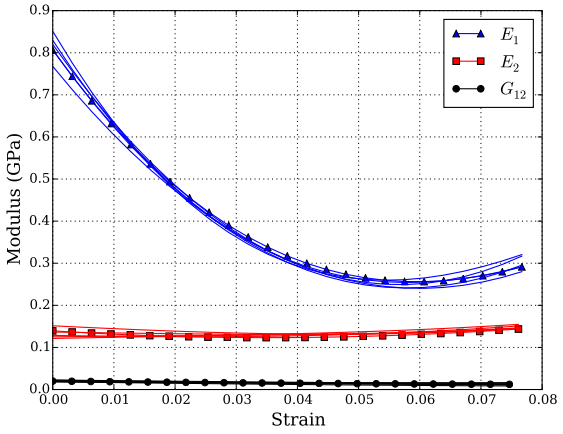

Fig. 10 Five best material models resulting from the optimization of 50 random starting points plotted alongside the assumed non-linear orthotropic material

non-linear orthotropic material. Two-dimensional plots of the node locations cut through the Y and X axes, as the material is inflated, are shown in Figs. 11 & 12. The node locations resulting from the 10 percent best found material models are plotted alongside the assumed solution. At the seven pressures, the node locations are analogous among the different material models. It can be further noted that the subtle variance in the best material models (seen in Fig. 10) is even less noticeable in the cut through plots of the FE bubble inflation models.

The inverse bubble inflation test was demonstrated to reproduce a highly non-linear material model from an assumed non-linear orthotropic material. However, obtaining the exact non-linear material model of the bubble inflation test posses to be a challenging optimization problem. This can be seen by the large num-

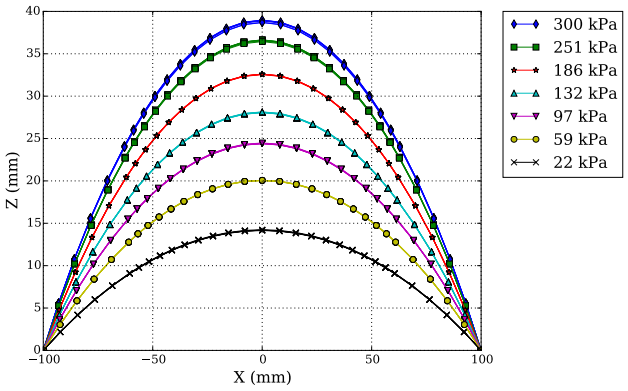

Fig. 11 Node locations cut through the Y axis from the FE bubble inflation models of the five best material models plotted alongside the assumed non-linear orthotropic material

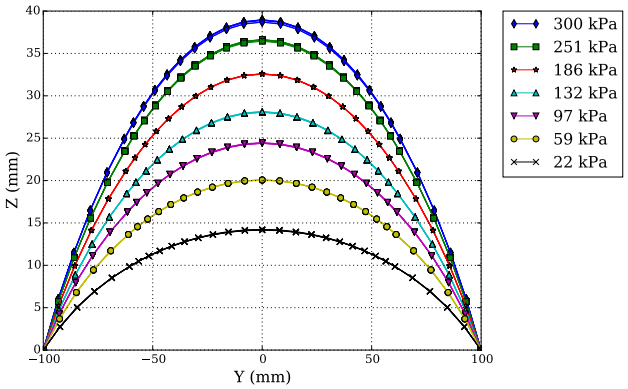

Fig. 12 Node locations cut through the X axis from the FE bubble inflation models of the five best material models plotted alongside the assumed non-linear orthotropic material

ber of local minimum discovered while not finding an objective function of zero.

6 Conclusion

An inverse bubble inflation test was performed from an assumed non-linear orthotropic material. It was demonstrated that the analysis produced non-linear material models similar to the assumed non-linear orthotropic material. Thus the inverse bubble inflation method is capable of obtaining non-linear orthotropic models from non-linear orthotropic materials. It is the intent of this inverse bubble inflation analysis to be used to characterize non-linear orthotropic models from physical bubble tests on a non-linear orthotropic material in the future. It was possible to determine the non-linear orthotropic model from the single bubble inflation load case with a non-linear orthotropic material. The inverse bubble inflation technique may be capable of characterizing other types of material models, on different types of materials where a thin shell or membrane assumption would be appropriate.

Polynomial surfaces were fitted to the nodal FE displacement results of the known material model. These polynomials are utilized as the solution in the formation of the objective function. Physical test data can be easily utilized in the current bubble inflation test setup. Polynomials can be fitted to the full displacement field data that one may obtain using a multi-camera DIC system.

The inverse bubble inflation test requires full displacement field matching. It was first attempted to obtain non-linear material models by matching the bubble shape, however this was unsuccessful. Many different material models were found to produce a similar bubble shape. Thus the nodal X, Y, and Z displacements are rather matched because the full displacement field response is unique to a particular material model.

The inverse method can be utilized to obtain non-linear orthotropic models from bubble inflation tests on a non-linear orthotropic material through gradient optimization. The performance of non-gradient based optimizations on the inverse bubble test, as well as other algorithms is still unknown. A simulation study can be performed on bubbles originating from shapes other than a circle to improve the effectiveness at characterizing a particular material parameter.

Acknowledgements Computations were performed using the University of Stellenbosch's Rhasatsha HPC: http://www.sun.ac.za/hpc

References

Ambroziak A, Kłosowski P (2014) Mechanical properties for preliminary design of structures made from PVC coated fabric. Construction and Building Materials 50:74–81, secondoftwo doi:10.1016/j.conbuildmat.2013.08.060

Cavallaro PV, Johnson ME, Sadegh AM (2003) Mechanics of plain-woven fabrics for inflated structures. Composite Structures 61(4):375–393, secondoftwo doi:10.1016/S0263-8223(03)00054-0

Charalambides M, Wanigasooriya L, Williams G, Chakrabarti S (2002) Biaxial deformation of dough using the bubble inflation technique. I. Experimental. Rheologica Acta 41(6):532–540, secondoftwo doi:10.1007/s00397-002-0242-2

Galliot C, Luchsinger R (2009) A simple model describing the non-linear biaxial tensile behaviour of PVC-coated polyester fabrics for use in finite element analysis. Composite Structures 90(4):438–447, secondoftwo doi:10.1016/j.compstruct.2009.04.016

Galliot C, Luchsinger RH (2011) Uniaxial and biaxial mechanical properties of ETFE foils. Polymer Testing 30(4):356–365, secondoftwo doi:10.1016/j.polymertesting.2011.02.004

Garbowski T, Maier G, Novati G (2011) On calibration of orthotropic elastic-plastic constitutive models for paper

foils by biaxial tests and inverse analyses. Structural and Multidisciplinary Optimization 46(1):111–128, secondoftwo doi:10.1007/s00158-011-0747-3

MSC Marc (2014) Volume A : Theory and User Information. MSC Software Corporation

Reuge N, Schmidt FM, Le Maoult Y, Rachik M, Abbé F (2001) Elastomer biaxial characterization using bubble inflation technique. I: Experimental investigations. Polymer Engineering and Science 41(3):522–531, secondoftwo doi:10.1002/pen.10749

Vanderplaats Research & Development Inc (2001) DOT Users manual, 5th edn. Colorado Springs, CO